



Article

Monitoring Land Use/Land Cover and Landscape Pattern Changes at a Local Scale: A Case Study of Pyongyang, North Korea

Yong Piao ¹, Yi Xiao ², Fengdi Ma ³, Sangjin Park ⁴, Dongkun Lee ⁵, Yongwon Mo ^{6,*}, Seunggyu Jeong ⁷, Injae Hwang ⁷ and Yujin Kim ⁷

- ¹ Interdisciplinary Program in Landscape Architecture and Integrated Major in Smart City Global Convergence, Seoul National University, Seoul 08826, Republic of Korea; topdyd@snu.ac.kr
- ² College of Landscape Architecture, Nanjing Forestry University, Nanjing 210037, China; shirley@njfu.edu.cn
- ³ Graduate School of Environmental Studies, Seoul National University, Seoul 08826, Republic of Korea; fengdima@snu.ac.kr
- ⁴ Korea Adaptation Center for Climate Change, Korea Environment Institute, Sejong 30147, Republic of Korea; parkssang87@snu.ac.kr
- ⁵ Department of Landscape Architecture and Rural System Engineering, Seoul National University, Seoul 08826, Republic of Korea; dklee7@snu.ac.kr
- ⁶ Department of Landscape Architecture, Yeungnam University, Gyeongsan 38541, Republic of Korea
- ⁷ Animal Resources Division, National Institute of Biological Resources, Incheon 222689, Republic of Korea
- * Correspondence: csmo12@yu.ac.kr; Tel.: +82-53-810-2979; Fax: +82-53-810-4660

Abstract: One method of understanding landscape pattern changes is through an understanding of land use/land cover (LULC) changes, which are closely related to landscape pattern changes. Previous studies have monitored LULC changes across North Korea but did not consider landscape changes at a local scale. Using multiple LULC products to construct sample points, the LULC was classified using a random-forest algorithm and Landsat satellite dataset. The overall accuracy of the classification was $97.66 \pm 1.36\%$, and the Kappa coefficient was 0.95 ± 0.03 . Based on the classification results, landscape indices were used to quantify and monitor landscape pattern changes. The results showed that, from 2000 to 2020, there was an increasing trend in built-up and forest areas in Pyongyang, while cropland showed a decreasing trend, and landscape fragmentation increased. However, urban expansion was not the main factor affecting fragmentation. The main factors were forest recovery and cropland reduction, leading to an increase in landscape fragmentation in Pyongyang.

Keywords: land use/land cover change; landscape pattern change; local scale; North Korea; remote sensing



Citation: Piao, Y.; Xiao, Y.; Ma, F.; Park, S.; Lee, D.; Mo, Y.; Jeong, S.; Hwang, I.; Kim, Y. Monitoring Land Use/Land Cover and Landscape Pattern Changes at a Local Scale: A Case Study of Pyongyang, North Korea. *Remote Sens.* **2023**, *15*, 1592. <https://doi.org/10.3390/rs15061592>

Academic Editors: Stanisław Lewiński and Wojciech Drzewiecki

Received: 17 January 2023

Revised: 9 March 2023

Accepted: 13 March 2023

Published: 15 March 2023



Copyright: © 2023 by the authors. Licensee MDPI, Basel, Switzerland. This article is an open access article distributed under the terms and conditions of the Creative Commons Attribution (CC BY) license (<https://creativecommons.org/licenses/by/4.0/>).

1. Introduction

Land use/land cover (LULC) data provide information on ecosystem services to humans with regard to food and other resources; however, in terms of spatial distribution, human activities in land use have led to changes in landscape patterns [1]. Altered landscape patterns are largely influenced by human activities and are associated with a decline in biodiversity, environmental pollution, soil degradation, and other issues [2]. Thus, understanding historical changes in landscape patterns is important for resolving these issues [3]. Landscape pattern changes can be reliably monitored through LULC changes because human land use directly affects these changes [4].

Moreover, land-use-change analysis assists in understanding landscape pattern changes. However, land-use-change analysis requires high-precision LULC datasets to improve the reliability of the results and closely monitor these changes [5]. LULC is widely used as the primary analysis data for studies on local climate zones [6], urban administration zones [7],

precinct ventilation zones [8], and urban functional zones [5,9]. The relationship between surface temperature and LULC in the heat island phenomenon is monitored based on LULC analysis at the urban scale [8,10–12]. Urban land expansion and population-transfer patterns can be analyzed based on LULC-change detection [9].

Several studies have been performed to better understand the relationship between land use and land cover change (LULC), urbanization, and landscape patterns. Specifically, analyzed urban land expansion and population-transfer patterns using LULC change detection [9] were used to investigate the relationship between LULC change, urbanization, and landscape patterns [13–15], as well as the relationship between urbanization and changes in agricultural landscape patterns [5]. To monitor these changes over time, it is important to regularly track LULC and landscape patterns because the spatial structure and distribution characteristics of LULC affect the monitoring of changes in landscape patterns [16,17].

The development and widespread use of remote-sensing tools and techniques facilitate the production of high-precision LULC data. Remote-sensing data provide historical information (including multi-temporal and spatial data) and various satellite products that can help effectively monitor and analyze LULC changes. Google Earth Engine (GEE) became accessible in 2017, considerably increasing the ease of conducting land-cover classification studies. GEE is a cloud-processing platform for satellite image data with the advantage of execution through code and on Google supercomputers, offering an integrated set of easy-to-use satellite data products that can markedly reduce the labor and time required for organizing, pre-processing, and analyzing data [18].

These features have significantly reduced the equipment requirements and thresholds required for remote-sensing studies. Several GEE-based LULC classification studies have been recently conducted. Among them, LULC results classified based on multi-source LULC products are highly reliable in terms of accuracy and visual interpretation [19–21]. The advantages of a classification approach using multi-source LULC products include its applicability to inaccessible areas, a considerable reduction of labor and time consumption, and the ability to provide highly accurate classification results.

Understanding how changes in LULC affect landscape patterns is important because changes in LULC lead to changes in landscape patterns [1]. Therefore, analyzing changes in land use helps to understand how landscape patterns change [13]. Monitoring and trend analysis of landscape pattern change can provide references for decision making at the planning level [17]. Information on compositional landscape change can be quantified through landscape metrics [7]. Landscape metrics are widely used in landscape pattern analysis to monitor spatial changes in landscape configuration and composition, providing information on changes, such as fragmentation, heterogeneity, and evenness [22].

Local-scale landscape pattern changes directly affect ecosystem service functions, and analyzing them can provide a valuable reference for environmental protection, sustainable urbanization, and ecological structure and function [16,17]. Hence, it is crucial to capture and monitor local-scale landscape pattern change. In this study, the spatial distribution of land cover, decreasing or increasing trends in land cover and landscape patterns, and changes in fragmentation and heterogeneity in Pyongyang were monitored based on the spatial structure and distribution characteristics of LULC data.

North Korea is inaccessible owing to its national policies, and, consequently, few studies provide information on the development trends and changes in the local urban area in Pyongyang, the capital of North Korea. Although some studies have examined the entire North Korean region [23], few have focused on the capital, Pyongyang, at a local scale. The main challenge in using LULC classification in such areas is the high heterogeneity and complexity of urban areas.

Furthermore, the landscape patterns in local areas in the capital in developing countries generally show a high degree of fragmentation, increasing heterogeneity, and discontinuity [7]. Therefore, understanding the characteristics of the study area and

selecting appropriate image analysis techniques and remote-sensing data are necessary [24].

North Korea has experienced various land-cover change related events since the 1980s. Beginning in the 1980s, deforestation in North Korea accelerated in magnitude as well as in form [25]. During this period, the area occupied by farmland in North Korea was expanding, and most of the flat ground and mountainous areas were reclaimed for agricultural use [26]. North Korea has since focused on environmental issues, such as deforestation. On 11 December 1992, North Korea officially enacted the Forest Law.

In June 2000 and October 2001, the Forest Law was strengthened through amendments and additions focusing on limiting terrace field expansion and deforestation. On 2 August 2005, afforestation, re-forestation, and logging restrictions were emphasized in the supplement to the Forest Law Amendment [27]. In addition, the implementation of the “10-year plan for forest restoration” is one of the main drivers of forest cover change. According to the “10-year plan for forest restoration” in North Korea, from 2013 to 2022, about 6.5 billion trees will be planted [28]. Based on the policy changes related to LULC, this study chose 10 year time intervals for analysis.

In this study, multi-source LULC products were used based on the time period and scale of the study area, and the optimal classification dataset and parameters were identified. We then used multi-source LULC products and Landsat time-series data for LULC classification based on a local-scale random-forest (RF) algorithm. High-precision time-series LULC result maps validated against confusion matrices and visual interpretation were used to monitor LULC and landscape pattern changes in Pyongyang. With respect to Pyongyang as the study area, building a reliable time-series LULC dataset in an inaccessible local area and providing information on the development and changes at the urban scale in North Korea are essential for reference and future research. To the best of our knowledge, no previous studies have examined landscape pattern changes in the capital of North Korea.

2. Study Area

North Korea (also known as the Democratic People’s Republic of Korea) is located in the northern part of the Korean Peninsula, bordering South Korea in the south and Russia and China in the north. It is located in a midlatitude temperate climate zone with four pronounced seasons (spring, summer, autumn, and winter). Spring and autumn are sunny and dry; summer is hot, cloudy and rainy; and winter is cold and dry. In North Korea, the flat terrain of the capital city, Pyongyang, is highly conducive to urban and agricultural development.

North Korea is a developing country where agriculture is a crucial economic sector, and the country is also facing a severe degradation of its forest resources [29]. Due to the mountainous topography that covers about 80% of the total area, the expansion of terraced fields has become necessary [28]. Due to political reasons, the city was originally built mainly in the northern areas of the Taedong River, which served as a defense line towards the south.

Later, in the process of rebuilding Pyongyang, North Korea expanded the urban area to the southern part of the Taedong River, resulting in the river running through the center of the city. As the primary urban hub of North Korea, the city’s population and economic growth are expected to drive the expansion of its built-up area. Despite this, the limited access to North Korea hinders the availability of literature and data concerning its cities and environment. Figure 1 shows the study area and its elevation based on the Shuttle Radar Topography Mission V3 product (SRTM3).

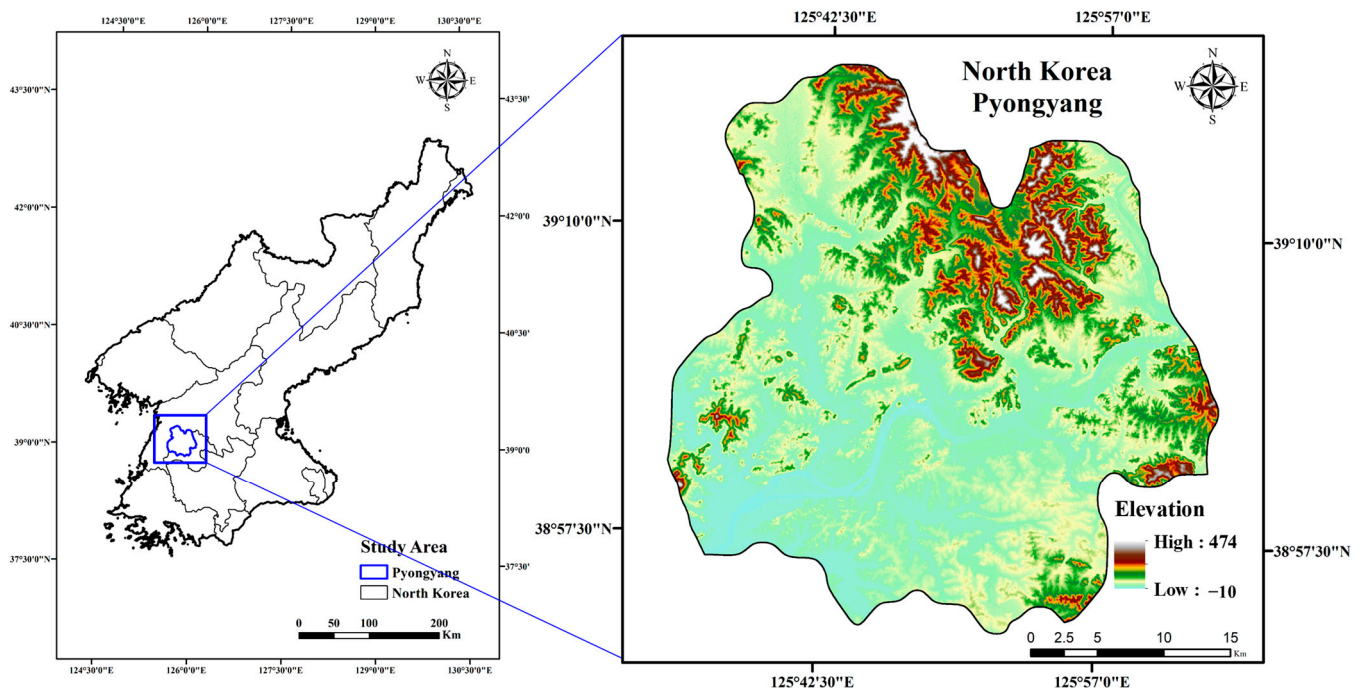


Figure 1. Study area: Pyongyang, North Korea (Democratic People’s Republic of Korea) with elevation.

3. Materials and Methods

Time-series land-cover classification was performed at the local scale, and LULC change detection and landscape pattern changes were analyzed (Figure 2) using four main steps. In the first step, semi-permanent sample points were constructed, and the satellite image dataset was pre-processed. In the second step, the semi-permanent sample points were randomly divided into training (70%) and testing (30%) datasets. The training dataset was used for classification, and the testing dataset was used to validate the classification results.

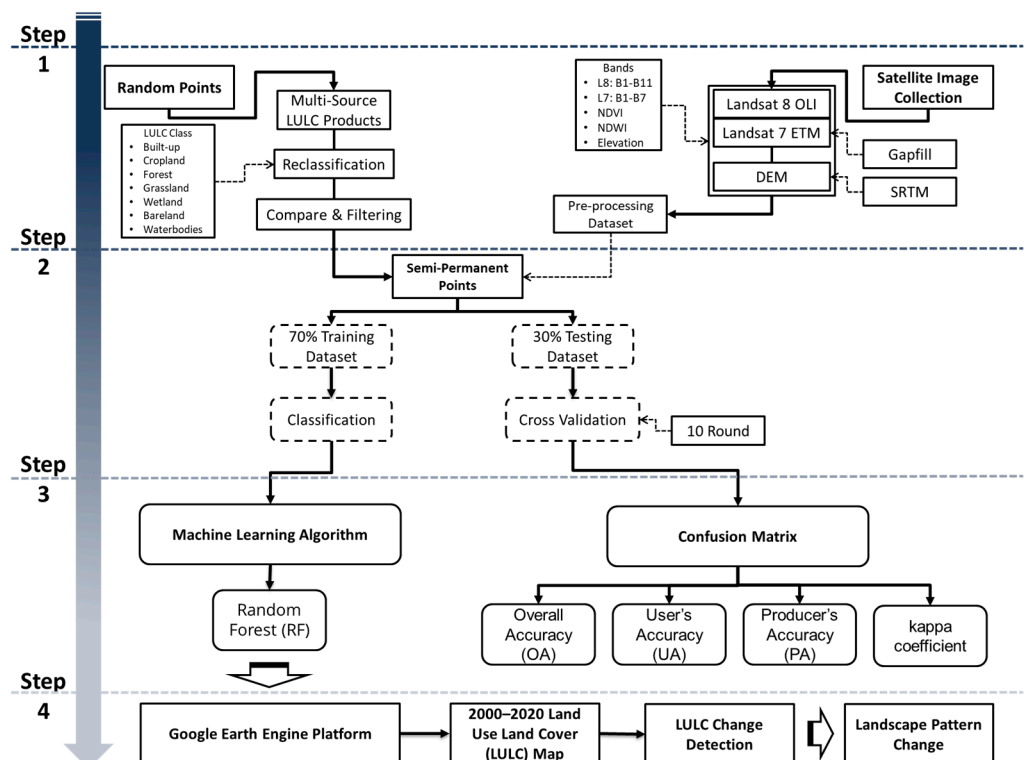


Figure 2. Research process flow chart.

Ten rounds of cross-validations were performed for the entire semi-permanent sample point dataset. In the third step, classification was performed based on a machine-learning algorithm and validated using a confusion matrix. In the fourth step, LULC change detection and landscape pattern changes were analyzed based on the LULC result maps. The first three steps of this study were performed on the GEE platform, a cloud platform for efficient processing and analysis of satellite data [18], and step 4 was performed using the ArcGIS platform.

3.1. Data Collection

This study analyzed LULC changes and trends in landscape pattern changes over a long-term time period from 2000 to 2020. Although there are products, such as Sentinel 2 (15 m), with higher resolution than Landsat (30 m), the availability of such products does not cover the research time period. Therefore, in this study, the Landsat 7 ETM+ Collection 2 Level 1 TOA and Landsat 8 OLI Collection 2 Level 1 TOA datasets were used for the classification dataset. In addition, the SRTM3, digital elevation data [30], and two satellite indices, the normalized difference vegetation index (NDVI) [31] and the normalized difference water index (NDWI) [32], were also included in each classification dataset.

Among them, we used satellite product time-series data from April–July 2000–2012, using data from 383 Landsat 7 images (2000: 28, 2001: 36, 2002: 28, 2003: 26, 2004: 26, 2005: 31, 2006: 33, 2007: 34, 2008: 33, 2009: 28, 2010: 25, 2011: 26, and 2012: 29) and 272 Landsat 8 images (2013: 10, 2014: 38, 2015: 41, 2016: 41, 2017: 36, 2018: 34, 2019: 35, and 2020: 37); data from a total of 655 images were used. After classification, the time-series LULC result map of the study area from 2000 to 2020 was obtained.

Among the multi-source LULC products, MODIS Land Cover Type Product MCD12Q1.006 [33], Copernicus Global Land Service Land Cover (CGLS-LC100) [34], the South Korean MoE LULC Product (egis.me.go.kr), Finer Resolution Observation and Monitoring of Global Land Cover (FROM-GLC) [35,36], GlobeLand30 (GLC30) [37], Global Forest Change dataset (GFCD) [38], and the global food security-support analysis data from southeast and northeast Asia (GFSAD30SEACE) [39] were used to construct sample points. Table 1 shows the data collection types, information, and references used in this study.

Table 1. Data collection types and information [30,33–39].

| Type | Data Collection | Used Temporal Coverage | Term | Spatial Resolution | Reference |
|-------------------|---|------------------------|---------|--------------------|---|
| Satellite Product | Landsat 7 ETM + Collection 2 Level 1 top-of-atmosphere reflectance (TOA) | 2000–2012 | 16 days | 30 m | (usgs.gov , accessed on 1 September 2022) |
| | Landsat 8 OLI Collection 2 Level 1 top-of-atmosphere reflectance (TOA) | 2013–2020 | 16 days | 30 m | (usgs.gov , accessed on 1 September 2022) |
| | Shuttle Radar Topography Mission V3 product (SRTM3) | 2000 | - | 30 m | Farr et al. [30] |
| LULC Product | MCD12Q1.006 | 2001–2020 | 1 year | 500 m | Sulla-Menashe & Friedl et al. [33] |
| | COPERNICUS | 2015–2019 | 1 year | 100 m | Masiliūnas et al. [34] |
| | South Korea’s Ministry of Environment (MoE) LULC Map | 2000, 2010 | - | 30 m | (egis.me.go.kr , accessed on 1 September 2022) |
| | Finer Resolution Observation and Monitoring of Global Land Cover (FROM-GLC) | 2015, 2017 | - | 30 m | Li et al. [35] Gong et al. [36] |

Table 1. Cont.

| Type | Data Collection | Used Temporal Coverage | Term | Spatial Resolution | Reference |
|------|---|------------------------|------|--------------------|----------------------|
| | GlobeLand30 (GLC30) | 2000, 2010, 2020 | - | 30 m | Chen et al. [37] |
| | Global Forest Change dataset (GFCD) | 2000 | - | 30 m | Hansen et al. [38] |
| | Global Food Security-support Analysis Data Extent Southeast and Northeast Asia (GFSAD30SEACE) | 2015 | - | 30 m | Oliphant et al. [39] |

3.2. Data Processing

Considering the geographical and climatic characteristics of the study area, identifying the appropriate period and removing noise were key to classification at the regional scale. The study area experiences four distinct seasons and is located in a semi-humid and semi-arid region with agriculture as the primary economic sector. In the Pyongyang region, the main agricultural activity is the annual cultivation of rice. Agricultural practices include planting and seeding from April to July/August with the tillering phase ending in July and the boosting/heading phase beginning in August.

Therefore, it is necessary to consider the timing of the growth and maturity periods of agricultural vegetation to avoid convergence with forest vegetation in the index [40]. The study area is located in a peninsular zone with cloudy and rainy summers, which also requires consideration to account for cloud data masking [23]. In Landsat products, the Surface Reflectance (SR) correction effect was reduced in the study area because it is located on the coast and in areas with extensive cloud noise. Through the classification comparison of the two products, we found that the SR product in the research area could not completely mask cloud noise. In this study, the Landsat-calibrated top-of-atmosphere (TOA) product [41] was used, and cloud-free synthetic data were created based on temporal aggregation methods, with a 3 year interdecadal window from April to July.

The salt-and-pepper noise was overcome through median synthesis, and a TOA synthetic dataset without cloud and salt-and-pepper noise in the study area was obtained [19,20]. Landsat Enhanced Thematic Mapper (ETM) 7 and Landsat 8 Operational Land Imager (OLI) were used for LULC classification from 2000 to 2020. The Landsat 7 dataset covered the time period 2000–2012, and the Landsat 8 dataset the time period 2013–2020. Landsat 7 products were gap-filled to correct the image data due to a severe failure of the Landsat 7 sensor from 2003 [42]. All Landsat datasets in this study were obtained from Collection 2.

It should be noted that the study area is inaccessible for policy reasons; thus, a verifiable and accurate classification method is needed. Based on previous studies, the classification approach using multi-source LULC products was used to apply time-series land-cover classification to the entire North Korean region [23]. This method is effective for time-series land-cover classification and validation of inaccessible areas for a wide range of applications in various regions [19–21,43], including alpine areas, extensive forests, and plains.

Seven existing LULC products were selected based on the methodological principles of “full consistency” and “temporal stability” [19]. Five of the LULC products had the same 30 m resolution as that of Landsat to reduce the uncertainty of evenness and geographical integrity [39]. To analyze and assess landscape pattern changes, we generated seven major land-cover categories based on the Ministry of Environment (MOE) classification system in Korea: built-up land, cropland, forest, grassland, wetland, bare land, and water bodies. We then constructed 10,000 random sample points in the study area and set the distance between the sampling points as >100 m to avoid accuracy deviation caused by excessively dense sampling points.

After extracting 10,000 sample points for each LULC type, inconsistent sample points were removed through an overlay analysis on other LULC products—that is, the filtered land-cover sample point attributes remained constant through annual variations over the study period. Here, we refer to filtered sample points as semi-permanent sample points. We overlaid the analysis of the randomly generated points with MCD12Q1, COPERNICUS, FROM-GLC, MOE LULC map, GLC30, GFCD, and GFSAD30SEACE to remove points that were “inconsistent” in the classification and obtained consistent points under multi-source LULC products.

Finally, from the 10,000 random data points, a total of 2767 semi-permanent sample points were filtered for land-cover classification. Based on the methodological principles of “full consistency” and “temporal stability,” unstable or extremely small land-cover classes cannot be filtered. We found that among the 2767 semi-permanent sample points, four LULC classes were present: built-up land, cropland, forest, and waterbodies. That is, the attributes of the semi-permanent sample points of these four filtered classes remained unchanged through annual variations over the study period. Finally, each Landsat spectral band, along with NDVI, NDWI, elevation, and sample points, were used for time-series classification from 2000 to 2020. Equation (1) was used to calculate the NDVI, and Equation (2) was used to calculate the NDWI.

$$NDVI = \frac{(NIR - Red)}{(NIR + Red)} \quad (1)$$

$$NDWI = \frac{(Green - NIR)}{(Green + NIR)} \quad (2)$$

In Landsat 8 OLI, NIR is band 5, red is band 4, and green is band 3. In Landsat 7, ETM and NIR are band 4, red is band 3, and green is band 2.

3.3. Machine-Learning Algorithm

In this study, classification was performed based on machine-learning algorithms that can overcome limitations, such as overfitting, and can use different subsets of the same training dataset [44]. The advantage of machine-learning algorithms lies in their nonparametric approach based on nonlinear data, which can improve classification accuracy by reducing covariance and noise handling in time-series data [45]. This study used the RF algorithm that was proposed by Breiman [46], a commonly used machine-learning algorithm. The RF algorithm is an ensemble-learning method for classification and regression analysis [47] and has been widely used for LULC classification [48] as it exhibits excellent performance [49].

RF includes bootstrap aggregation (termed bagging) and random feature selection. In RF, multiple samples extracted by bagging the training samples are combined with a classification tree and predicted by a voting process [46]. Based on a previous study [50], the number of decision trees was set to 500, which was confirmed to be adequate for classification. The 2767 semi-permanent sample points were randomly divided into training (70%) and test (30%) datasets according to the LULC classes (built-up land, cropland, forest, and waterbodies).

The training dataset was used for classification, and the test dataset was used to verify the classification results. Accuracy validation uses a confusion matrix with four accuracy metrics for verification: the overall accuracy, consumer accuracy, producer accuracy, and kappa coefficient. To improve the reliability of the classification results, the LULC results were cross-validated 10 times based on the cross-validation method—that is, 10 rounds of cross-validations were performed for the entire 2767 semi-permanent sample point dataset. The validation values were the mean and standard deviation of the accuracy indicators from 2000 to 2020.

3.4. LULC Change Detection

Based on the classification result map, spatial analysis was performed to detect the trend of LULC-type changes in the study area and produce an LULC spatial conversion map. The time-series land-cover classification maps from 2000 to 2020 were analyzed for 2000–2010 and 2010–2020. LULC change detection and spatial conversion map generation were achieved by overlaying the classification result maps for the two specific periods. The 10 year intervals of 2000–2010 and 2010–2020 were chosen based on the time course of deforestation and forest protection activities in North Korea. The proportion of area and changes in each LULC category in the study area were analyzed from the classification result maps using Equations (3) and (4).

The proportion of each LULC type used was calculated as follows:

$$A_i\% = \frac{A_i}{A_t} \times 100\% \quad (3)$$

The change for each LULC type was calculated as follows:

$$A_i = A_{it1} - A_{it2}, \quad (4)$$

where A_i is the area of the LULC type i , A_t is the total area of the study area, and $A_i\%$ is the proportion of area of the LULC type i . $t1$ and $t2$ are two specific periods, and A_{it1} and A_{it2} are the total area of the LULC type i for specific periods $t1$ and $t2$, respectively.

3.5. Landscape Metrics for Landscape Pattern Changes

LULC changes are a part of the landscape elements that lead to changes in landscape patterns, and monitoring changes in landscape patterns in the study area is important for sustainable landscape planning [51]. Landscape metrics have been widely used to assess LULC and changes in landscape patterns [24].

To study the fragmentation and heterogeneity of landscape patterns in the study area, the following factors were selected at the local level: number of patches (NP), largest patch index (LPI), landscape shape index (LSI), and Shannon's evenness index (SHEI); and at the class level: NP, patch density (PD), LPI, percentage of landscape of class (PLAND), and perimeter area fractal dimension (PAFRAC).

To analyze the landscape composition, NP and PD metrics were used to analyze fragmentation according to the area and density of each land cover type. To analyze the configuration of the landscape pattern, LPI, LSI, PLAND, SHEI, and PAFRAC metrics were used to analyze the heterogeneity and evenness of the landscape according to the distribution, shape, and size of land cover. All landscape pattern analyses were performed using FRAGSTATS 4.2, a spatial pattern analysis program for quantifying landscape structure [22]. Table 2 shows the landscape metric information used for analyzing landscape pattern changes. The equations for calculating these metrics are as follows [22]:

The patch density was calculated as follows:

$$PD = \frac{NP}{A} \times 10,000 \times 100, \quad (5)$$

where NP is the number of patches, and A is the total landscape area (m^2); $0 < PD \leq 1 \times 10^6$.

The largest patch index was calculated as follows:

$$LPI = \frac{\max_{j=1}^n(a_{ij})}{A} \times 100 \quad (6)$$

where $\max(a_{ij})$ is the area of the patch (m^2), and A is the total landscape area (m^2); $0 < LPI \leq 100$.

The landscape shape index was calculated as follows:

$$LSI = \frac{E}{\min E}, \quad (7)$$

where E is the total edge length on cell surfaces, and $\min E$ is the minimum total edge length on cell surfaces; $LSI \geq 1$.

The percentage of landscape of class was calculated as follows:

$$PLAND = \frac{\sum_{j=1}^n a_{ij}}{A} \times 100, \quad (8)$$

where a_{ij} is the area of each patch, and A denotes the total landscape area; $0 < PLAND \leq 100$.

The Shannon evenness index was calculated as follows:

$$SHEI = \frac{-\sum_{i=1}^m (P_i \times \ln P_i)}{\ln m}, \quad (9)$$

where P_i is the proportion of class, and m is the number of classes; $0 \leq SHEI < 1$.

The perimeter area fractal dimension was calculated as follows:

$$PAFRAC = \frac{2}{\beta} \quad (10)$$

where β is the slope of the regression of the area against the perimeter (logarithm); $1 \leq PAFRAC \leq 2$.

Table 2. Landscape metric type information used at the local and class levels in Pyongyang.

| Landscape Metrics | Abbreviation | Description | Range | Local Level | Class Level |
|----------------------------------|--------------|--|-------------------------|-------------|-------------|
| Number of patches | NP | The number of patches | $NP \geq 1$ | O | O |
| Patch density | PD | The aggregation of different LULC types in the landscape | $PD \leq 1 \times 10^6$ | | O |
| Largest patch index | LPI | The percentage of landscape covered by the corresponding largest patch for LULC class type | $0 < LPI \leq 100$ | O | O |
| Landscape shape index | LSI | The ratio between the actual landscape edge length and the assumed minimum edge length | $LSI \geq 1$ | O | |
| Percentage of landscape of class | PLAND | The proportion of total area occupied by the LULC class type | $PLAND \leq 100$ | | O |
| Shannon's evenness index | SHEI | A measure of patch diversity, determined by the proportional distribution of different LULC types in the landscape | $0 \leq SHEI < 1$ | O | |
| Perimeter area fractal dimension | PAFRAC | A measure of shape, determined by the patch complexity of LULC class type in landscapes | $1 \leq PAFRAC \leq 2$ | | O |

4. Results

4.1. LULC Classification Results and Accuracy

Figure 3 shows a map of the land-cover classification results for the study area from 2000 to 2020. After extracting 10,000 sample points for each LULC type (built-up, cropland, forest, grassland, wetland, bareland, and waterbodies), points were identified that have the same classification attributes through multi-source LULC products, yielding sample points that remain constant over the annual variation of the study period. These we refer to as semi-permanent sample points.

Based on the filtering of semi-permanent sample points, four classes were obtained in the LULC major category: built-up land, cropland, forest, and waterbodies. This can be attributed to Pyongyang's location and agricultural activities. Pyongyang is located in the

interior of the peninsula, and most of the flat land and forest areas have been reclaimed as agricultural land and terraced fields [26]. Therefore, in the Pyongyang region, unstable or extremely small land-cover classes could not be filtered.

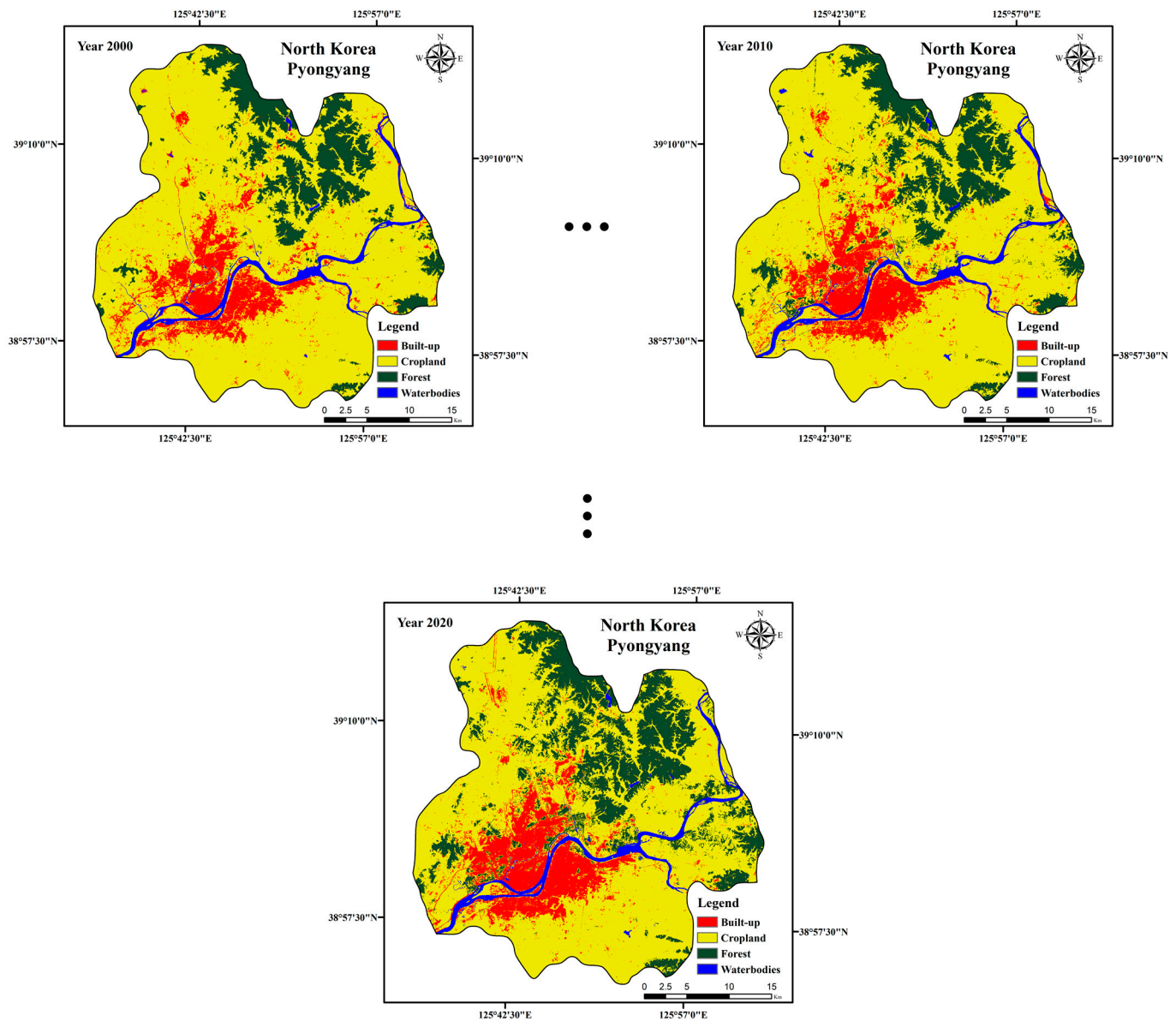


Figure 3. The time series LULC classification results from 2000 to 2020; Details based on 10 years as a period for 2000, 2010, and 2020.

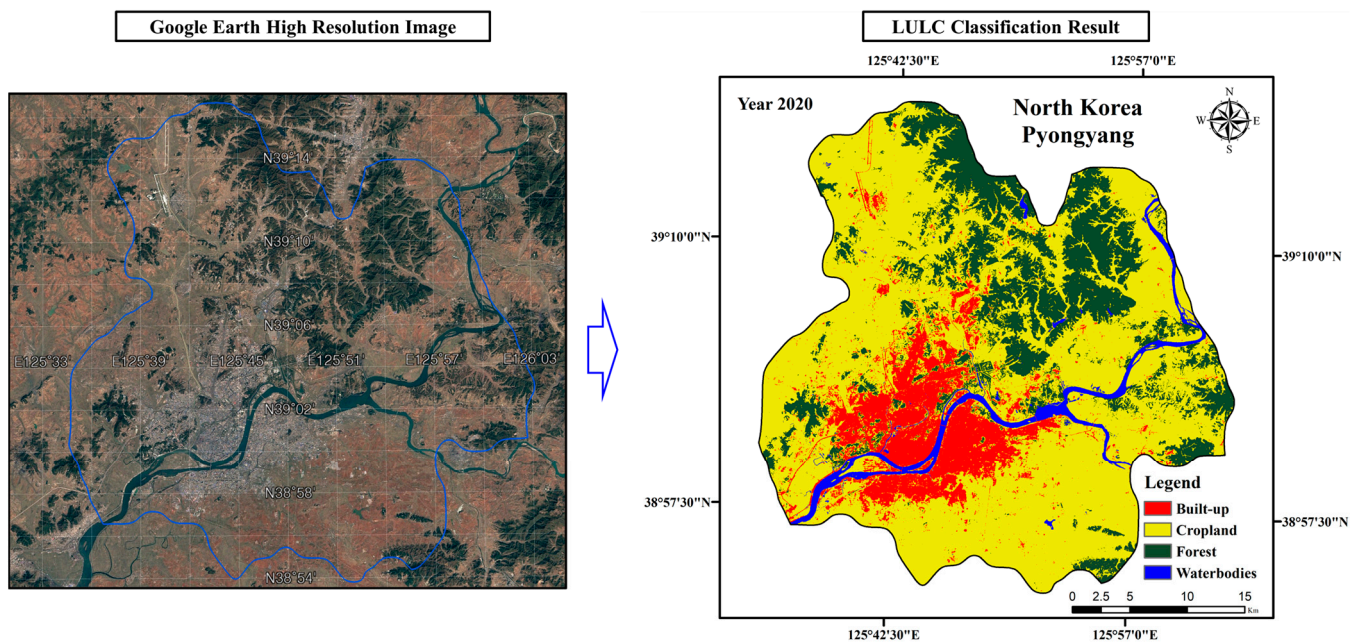
A total of 10 rounds of cross-validation were performed on the LULC results, and the validation values are presented as the mean and standard deviation of the 2000–2020 accuracy metrics. Table 3 presents the range of the accuracy metrics for the classification results from 2000 to 2020. The overall accuracy of the classification results was $97.66 \pm 1.36\%$, and the Kappa coefficient was 0.95 ± 0.03 .

The consumer accuracies for the built-up area, cropland, forest, and waterbodies were $96.56 \pm 3.44\%$, $98.29 \pm 1.71\%$, $99.30 \pm 0.70\%$, and $100 \pm 0\%$, respectively, and the producer accuracies were $92.06 \pm 3.89\%$, $99.05 \pm 0.95\%$, $98.55 \pm 1.45\%$, and $98.21 \pm 1.79\%$, respectively. These results indicate that the classification results were highly accurate and that the precision met the criteria specified in the U.S. Geological Survey (USGS) classification scheme [52]; hence, they were used in the next step of the landscape pattern change analysis.

Table 3. Accuracy of the LULC classification results for 2000–2020.

| Land Cover | User Accuracy | Producer Accuracy |
|------------------|---------------|----------------------------------|
| Built-up | 96.56 ± 3.44% | 92.06 ± 3.89% |
| Cropland | 98.29 ± 1.71% | 99.05 ± 0.95% |
| Forest | 99.30 ± 0.70% | 98.55 ± 1.45% |
| Waterbodies | 100 ± 0% | 98.21 ± 1.79% |
| Overall Accuracy | 97.66 ± 1.36% | Kappa Coefficient 0.95 ± 0.03 |

In addition, Google Earth high-resolution images were used to compare the visual interpretation of the LULC classification result map to improve the reliability of the overall classification. Figure 4 shows the visual interpretation of the classification result map of the study area in 2020 compared with the Google Earth high-resolution image. The four generated land-cover types were highly similar to those found in the actual high-resolution image and were, therefore, used as data for further analyses.

**Figure 4.** Visualizing interpretation compared with a Google Earth high-resolution image from 2020.

4.2. LULC Change-Detection Results

Figure 5 shows the land cover change maps of the study area from 2000 to 2010 and 2010 to 2020. On the whole, the built-up area expanded from 2000 to 2020, mainly from the main urban area. The forest showed some recovery in various parts of the region from 2000 to 2010, and a clear recovery trend was found from 2010 to 2020. Although cropland showed some changes from 2000 to 2010, there are no obvious changes in the mountainous areas of the northeast from 2010 to 2020, and the main changes are concentrated in the outer areas of the main urban area.

Figure 6 shows, in detail, the land cover spatial transformation map of the study area from 2000 to 2010 and 2010 to 2020. Combined with Figure 5, we find that urbanization mainly transforms cropland, and this transformation is clear from 2000 to 2020. As the capital city of North Korea, Pyongyang shows an obvious trend in built-up expansion, and the cropland around the urban area that was originally used for agricultural production has become urbanized. In addition, we found that the transition from cropland to forest was clear from 2010 to 2020.

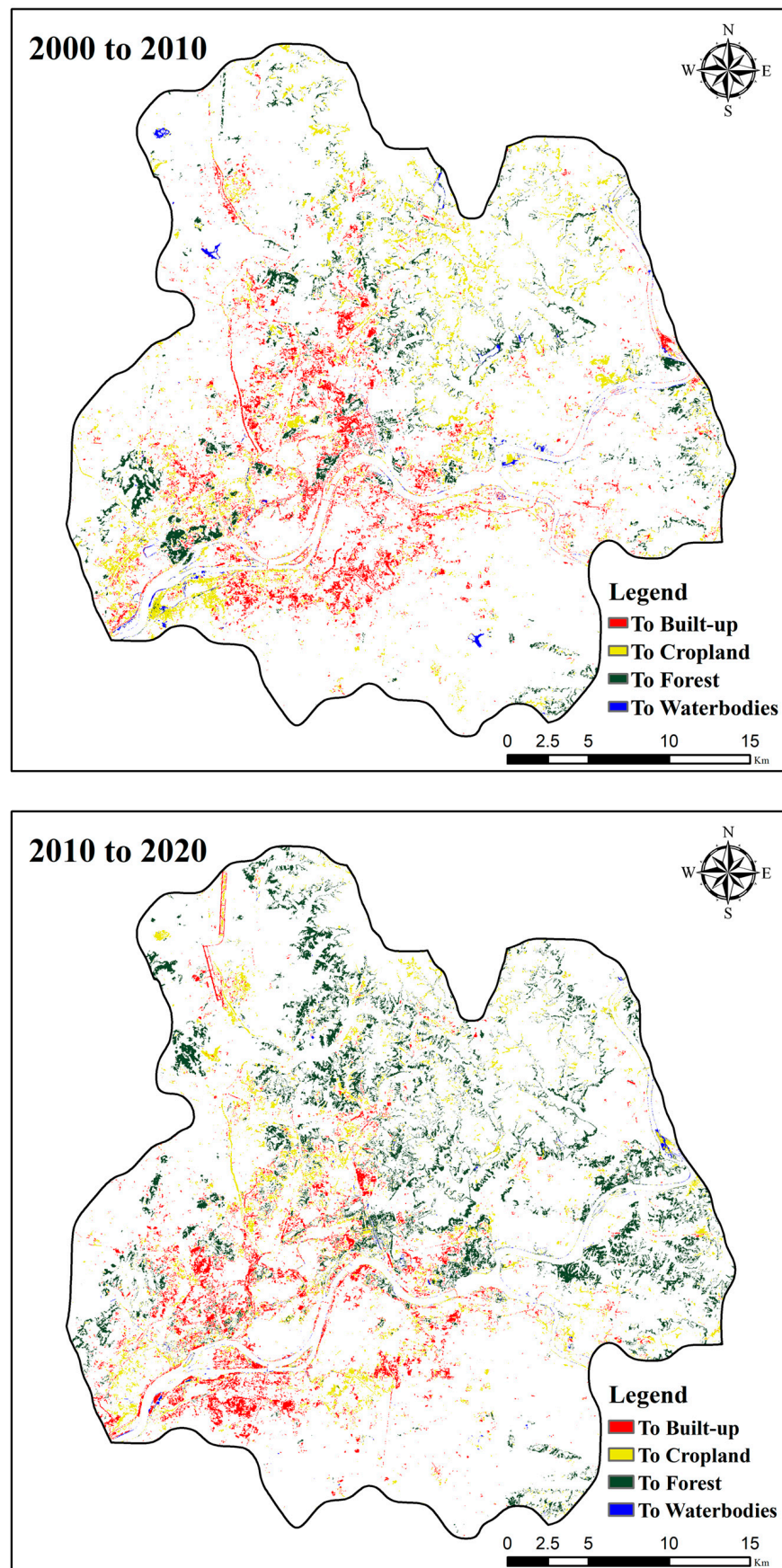


Figure 5. Land cover change maps for 2000–2010 and 2010–2020.

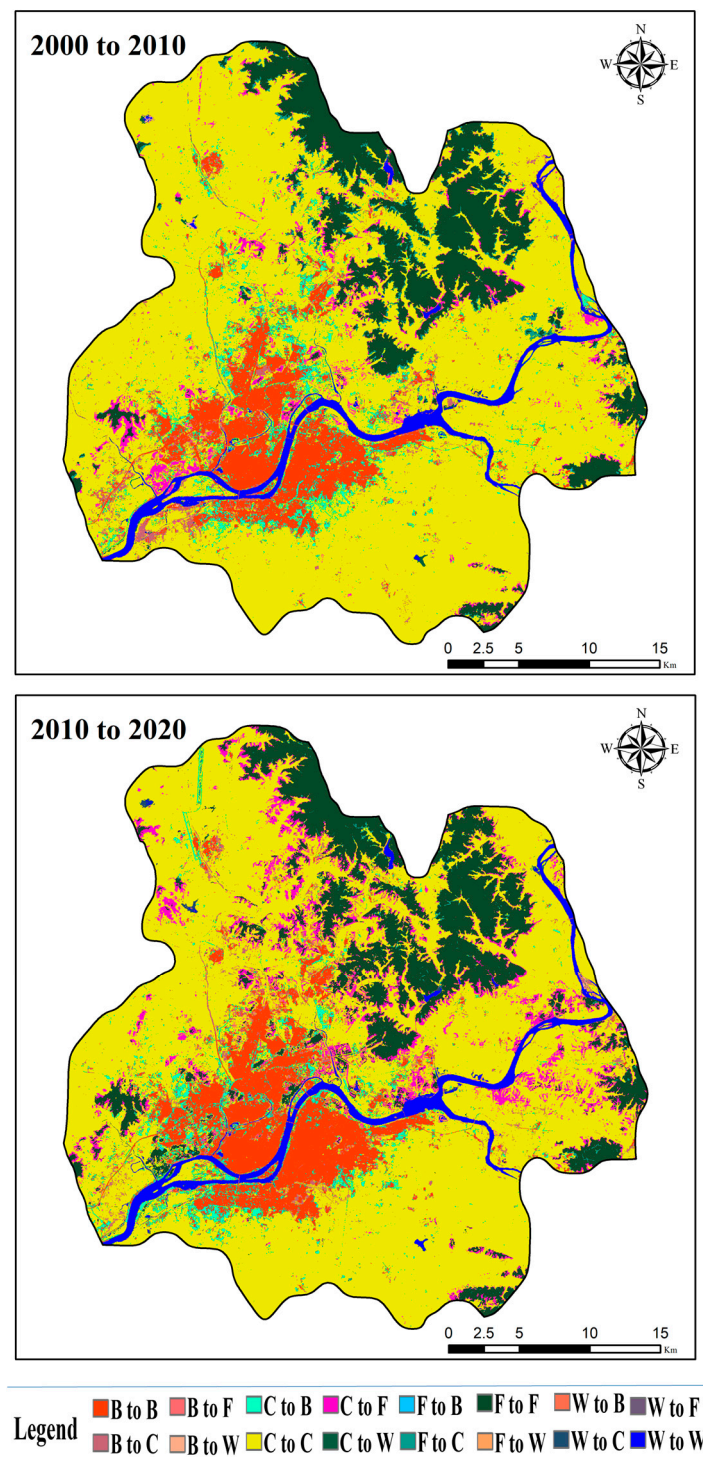


Figure 6. Spatial transformation maps for 2000–2010 and 2010–2020. B: built-up; C: cropland; F: forest; and W: waterbodies.

In terms of space, the transformation mainly occurs at the edge of mountainous areas, such as the east, northeast, and west, indicating terraced fields, which are one of the agricultural characteristics of North Korea being restored to forest. This can be attributed to the amendments to the North Korea Forest Law and the implementation of the “10-year plan for forest restoration” [28].

From 2000 to 2010, the transformation from cropland to forest was not obvious; however, from 2010 to 2020, the implementation of the amended Forest Law began to show distinct forest protection effects. Corresponding to the mountain agriculture terrace field,

the strengthening of forest protection has led to the fact that the terraced field is no longer an expanding form of agriculture, and many terraced fields have begun to be abandoned or are not expanding. North Korea's "10-year plan for forest restoration" afforestation program started in 2013 and will plant about 6.5 billion trees by 2022 [28]. This is also consistent with the trend in transformation from cropland to forest between 2010 and 2020.

Table 4 shows the rate of change in the area of each land-cover type from 2000 to 2010 and from 2010 to 2020. The built-up area increased from 8.26% to 9.49%, the cropland area decreased from 66.68% to 61.31%, the forest area increased from 11.96% to 14.17%, and waterbodies increased from 3.08% to 3.10%. Overall, this is consistent with the land-cover change, and conversion trends are shown in Figures 5 and 6. Built-up areas and forests both showed increasing trends, cropland showed a decreasing trend, and waterbodies did not change significantly.

Table 4. Area change ratios of land-cover types in 2000–2010 and 2010–2020.

| | Land Cover | Built-Up | Cropland | Forest | Waterbodies |
|--------------|-------------|----------|----------|--------|-------------|
| 2000 to 2010 | Built-up | 8.26% | 2.13% | 0.02% | 0.09% |
| | Cropland | 3.33% | 66.68% | 2.78% | 0.20% |
| | Forest | 0.00% | 1.32% | 11.96% | 0.00% |
| | Waterbodies | 0.09% | 0.06% | 0.00% | 3.08% |
| Total (%) | | | 100% | | |
| 2010 to 2020 | Built-up | 9.49% | 2.06% | 0.05% | 0.08% |
| | Cropland | 2.93% | 61.31% | 5.87% | 0.07% |
| | Forest | 0.02% | 0.56% | 14.17% | 0.01% |
| | Waterbodies | 0.06% | 0.19% | 0.02% | 3.10% |
| Total (%) | | | 100% | | |

4.3. Landscape Pattern Change

To study the fragmentation and heterogeneity of landscape patterns, NP, LPI, LSI, and SHEI were selected at the local level, whereas NP, PD, LPI, PLAND, and PAFRAC were selected at the class level. As shown in Table 5, From 2000 to 2020, NP increased from 9304 to 16,538, indicating increasing fragmentation of the Pyongyang landscape. The LPI decreased from 18.53% to 15.33%, indicating that the maximum patch area at the landscape scale gradually decreased. The increase in SHEI from 0.61 to 0.71 indicates that the evenness of the Pyongyang landscape increased, whereas the NP and LPI suggests that the landscape fragmentation in Pyongyang also increased. The corresponding LSI and SHEI increased, and heterogeneity, and evenness also increased.

Table 5. Landscape pattern changes at the local level in Pyongyang, North Korea.

| Local Level | | Landscape Metrics | | |
|-------------|--------|-------------------|-------|------|
| Year | NP | LPI | LSI | SHEI |
| 2000 | 9304 | 18.53% | 22.85 | 0.61 |
| 2010 | 11,559 | 17.88% | 27.65 | 0.65 |
| 2020 | 16,538 | 15.33% | 34.84 | 0.71 |

Table 6 shows the changes in landscape patterns in the study area from 2000 to 2020 at the class level. Built-up area, cropland, and forest landscape patterns changed significantly, whereas changes in waterbodies were not significant.

The NP of built-up areas increased from 5167 to 5829 and then decreased to 5768 from 2000 to 2020; although there was a decrease in NP from 2010 to 2020, it was not significant. The increase in PD from 1.87% to 2.08% is also consistent with the increase in fragmentation. PAFRAC decreased from 1.32 to 1.26, indicating that built-up areas were expanding in a progressively regularized form.

Table 6. Landscape pattern changes at the class level in Pyongyang, North Korea.

| Class Level | | Class Metrics | | | | |
|-------------|-------------|---------------|-------|--------|--------|--------|
| Year | Class | NP | PD | LPI | PLAND | PAFRAC |
| 2000 | Built-up | 5167 | 1.87% | 1.72% | 4.45% | 1.32 |
| 2010 | Built-up | 5829 | 2.11% | 3.19% | 4.96% | 1.34 |
| 2020 | Built-up | 5768 | 2.08% | 4.07% | 5.31% | 1.26 |
| 2000 | Cropland | 2450 | 0.89% | 18.53% | 30.99% | 1.28 |
| 2010 | Cropland | 2743 | 0.99% | 17.88% | 29.80% | 1.32 |
| 2020 | Cropland | 5768 | 2.08% | 15.33% | 27.22% | 1.32 |
| 2000 | Forest | 1324 | 0.48% | 1.87% | 5.64% | 1.27 |
| 2010 | Forest | 2641 | 0.95% | 2.53% | 6.27% | 1.30 |
| 2020 | Forest | 4464 | 1.61% | 1.74% | 8.54% | 1.32 |
| 2000 | Waterbodies | 363 | 0.13% | 1.22% | 1.37% | 1.37 |
| 2010 | Waterbodies | 346 | 0.13% | 0.71% | 1.43% | 1.38 |
| 2020 | Waterbodies | 538 | 0.19% | 0.62% | 1.39% | 1.32 |

The NP of cropland increased from 2450 to 5768, and PD increased from 0.89% to 2.08%, indicating that fragmentation was severe and had increased. The LPI decreased from 18.52% to 15.33%, and PLAND decreased from 30.99% to 27.22%, indicating that the cropland area gradually decreased, and fragmentation increased, which is consistent with the LULC change detection discussed above in Section 4.2. The PAFRAC increased from 1.28 to 1.32, indicating that the reduction in cropland area and fragmentation caused cropland to become more complex in shape. Combined with the results shown in Figure 5, this also indicates that forest recovery led to the spatial transformation of cropland, which tended to exhibit fragmentation.

The NP of forests increased from 1324 to 4464, and PD increased from 0.48% to 1.61%, indicating that fragmentation was severe and gradually increased. The LPI increased from 1.87% to 2.53% and then decreased to 1.74%, and the PLAND increased from 5.64% to 8.54%. The increase in PAFRAC (1.5%) indicates that the reclaimed forest from 2000 to 2010 was rehabilitated in multiple locations from 2010 to 2020, resulting in an increasing trend in the overall forest area despite the decrease in the area of major patches. The increase in PAFRAC (from 1.27 to 1.32) also indicates the spatial distribution and growth of forests, resulting in a complex shape.

5. Discussion

Pyongyang, the capital city of North Korea, experienced pronounced changes, such as city expansion and forest restoration, from 2000 to 2020. The main LULC changes observed in Pyongyang are urban expansion and forest restoration. Both changes are largely correlated with cropland conversion. Forest restoration primarily occurred between 2010 and 2020, with a focus on suburban and mountainous regions. This suggests that terraced fields were converted to forests as a result of afforestation policies.

The spatial impacts of these changes have led to increased regional fragmentation, with forest restoration and reduction in cropland being the primary drivers. From 2000 to 2010, the built-up area in Pyongyang exhibited fragmented increase, followed by a period of stabilization from 2010 to 2020 with a slight decrease in the degree of fragmentation. Conversely, during the same time period, the development of the main urban area of Pyongyang became more compact, indicating that urban expansion is not the primary factor affecting fragmentation.

Specifically, the percentage of the built-up area increased from 8.26% to 9.49%, with a total increase of 1.26%. The spatial analysis of LULC changes revealed a clear trend of an outward expansion of the built-up area in the main urban area. According to the Major Statistical Indicators of North Korea [53], the total population of Pyongyang increased from 2,777,000 in 2000 to 3,084,000 in 2020, and the urbanization rate increased from 59.412

in 2000 to 62.381 in 2020. This is consistent with the growth trend of built-up areas and expansion of the main urban area of Pyongyang. The cropland area decreased from 66.68% to 61.31%, with a total decrease of 5.37%.

The forest cover increased from 11.96% to 14.17%, with a total increase of 2.21%. From 2000 to 2010, the conversion of cropland to forest was 2.78%, and that of forest to cropland was 1.78%; the forest-to-cropland conversion was 1.32%. However, from 2010 to 2020, cropland-to-forest conversion was 5.87%, whereas forest-to-cropland conversion was only 0.56%. This indicates that there was no significant forest-to-cropland conversion trend from 2010 to 2020, whereas a significant cropland-to-forest conversion was observed, and the forest recovery trend was pronounced.

Corresponding to the spatial transformation map of LULC changes, the cropland was converted to forest throughout Pyongyang between 2010 and 2020. According to the North Korean Industrial Statistics [54], agricultural production in North Korea is a key source of economic income, and the flat terrain areas in Pyongyang are well-suited for the reclamation and expansion of cropland. As cropland serves as the main income and livelihood of North Korea, deforestation and terracing are practiced [28].

North Korea has recently been focusing on enhancing forest protection [27], and Pyongyang has a high capacity for economic development and policy implementation [55]. The formal enactment of the Forest Law in 1992, the additions and amendments to the Forest Law in 2001 and 2005 [28], and the reported success of the afforestation industry in North Korea in 2013 [56] are consistent with the observed LULC trends and the LULC spatial transformation map.

A distinct change in the landscape pattern in Pyongyang was observed from 2000 to 2020. At the landscape level, NP increased from 9304 to 16,538, with a total increase of 7234, and LPI decreased from 18.53% to 15.33%, with a total decrease of 3.2%. Overall, NP showed a distinct increasing trend, whereas LPI showed a decreasing trend, indicating severe fragmentation. Cropland NP showed an increasing trend from 2450 to 5768, with a significant area reduction in the largest patch. This could be attributed to the Forest Law and the outward expansion of the main urban area in Pyongyang, which increased the degree of cropland fragmentation.

Correspondingly, forest NP increased from 1324 to 4464, and forest fragmentation also increased. Analysis of LSI and SHEI at the landscape level revealed that LSI increased from 22.85 to 34.84 and SHEI increased from 0.61 to 0.71—that is, the increase in heterogeneity and evenness indicates the fragmentation trend of forest and cropland. At the class level, PAFRAC decreased from 1.32 to 1.26 in built-up areas, increased from 1.28 to 1.32 in cropland, and increased from 1.27 to 1.32 in forest land, indicating that the built-up area had a simplified shape under human influence, whereas the shape of forest and cropland tended to be complex.

In general, the outward expansion of the main urban area in Pyongyang during the 20 year study period led to the conversion of a portion of cropland to built-up land, and the growth and expansion of the city during this period led to changes in the natural ecosystem services of the area, resulting in a more fragmented landscape pattern. According to the NP, LPI, LSI, and SHEI landscape metrics, Pyongyang showed a high degree of fragmentation, and the heterogeneity tended to increase. The reduction in cropland and restoration of forests had clear impacts on the landscape heterogeneity. In the landscape pattern analysis at the class level, built-up areas were more aggregated, and the fragmentation and heterogeneity of forest and cropland increased.

One limitation of this study was that, due to the relative inaccessibility of North Korea, it was not possible to verify these findings on the ground. This same fact, however, highlights the importance of the present study as one of the few ways of monitoring land-use changes in inaccessible regions.

6. Conclusions

In this study, we quantified the landscape pattern changes in Pyongyang from 2000 to 2020. Sample points were constructed using multi-source LULC products, and LULC classification was performed based on the random-forest algorithm and remote-sensing data. The classification results were verified using confusion matrices and visual interpretations. Based on the LULC result map, the landscape pattern was quantified and monitored using landscape metrics. The landscape metrics used at the local level included NP, LPI, LSI, and SHEI, and, at the class level, NP, PD, LPI, PLAND, and PAFRAC were used.

Spatial scale is one of the key factors in landscape ecology. The landscape pattern depends on the scale, and the resolution, accuracy, and continuity of LULC used for analysis can affect the monitoring results. Consistent and continuous LULC classification results can stably monitor trends in landscape pattern changes without excessive fluctuations of abnormal values. The results of the analysis show that forest restoration and a decrease in cropland were mainly responsible for the intensification of fragmentation in Pyongyang's landscape, while the expansion of the city was not the main factor affecting fragmentation.

We observed that the development of Pyongyang has the following characteristics:

1. The flat ground areas have been fully utilized, allowing for ample room for future development.
2. The main urban area has been developed in a compact manner, which is beneficial in slowing down the trend of urban fragmentation.
3. The expansion of the main urban area has resulted in the conversion of surrounding cropland into built-up areas, and making full use of the landscape resources of the Taedong River.

In addition, there has been a noticeable restoration of forests in the eastern region; however, these tend to be dispersed and fragmented, which has adverse effects on the ecological environment. However, simply understanding the trends of land-use change and the trends of fragmentation in the landscape pattern is not sufficient. To make appropriate sustainable development plans, it is necessary to understand the causes of LULC change. The lack of literature and data due to political reasons in North Korea does not allow for an analysis of the main drivers and causes of changes in space. In the future, analysis at the spatial dimension or comparison with South Korea, which has a similar geography and climate should be performed to fully explore the factors influencing the changes.

Author Contributions: Conceptualization, Y.P.; Methodology, Y.P.; Validation, Y.P. and F.M.; Formal analysis, Y.P., Y.X. and F.M.; Data curation, Y.X. and F.M.; Writing—original draft, Y.P.; Writing—review & editing, S.P., D.L., Y.M. and S.J.; Visualization, Y.X. and S.P.; Supervision, D.L. and Y.M.; Project administration, S.J., I.H. and Y.K.; Funding acquisition, S.J., I.H. and Y.K. All authors have read and agreed to the published version of the manuscript.

Funding: This work was supported by a grant from the National Institute of Biological Resources (NIBR), funded by the Ministry of Environment (MOE) of the Republic of Korea (NIBR202203114). This work was also supported by the 2020 Yeungnam University Research Grant.

Data Availability Statement: The data that support the findings of this study are available on request from the corresponding author.

Acknowledgments: We acknowledge the anonymous reviewers and editors for reviewing this paper. The suggestions and comments of anonymous reviewers and editors have greatly improved the overall quality of the paper. The authors would also like to acknowledge Google Earth Engine platforms (GEE) through which the data/products were accessed and analyzed for the present study. All authors contributed to the development of this work.

Conflicts of Interest: The authors declare no conflict of interest.

References

1. Lambin, E.F.; Turner, B.L.; Geist, H.J.; Agbola, S.B.; Angelsen, A.; Bruce, J.W.; Coomes, O.T.; Dirzo, R.; Fischer, G.; Folke, C.; et al. The causes of land-use and land-cover change: Moving beyond the myths. *Glob. Environ. Change* **2001**, *11*, 261–269. [CrossRef]
2. Vitousek, P.M.; Mooney, H.A.; Lubchenco, J.; Melillo, J.M. Human domination of Earth's ecosystems. *Science* **1997**, *277*, 494–499. [CrossRef]
3. Braimoh, A.K. Random and systematic land-cover transitions in northern Ghana. *Agric. Ecosyst. Environ.* **2006**, *113*, 254–263. [CrossRef]
4. Yang, X.; Zheng, X.-Q.; Chen, R. A land use change model: Integrating landscape pattern indexes and Markov-CA. *Ecol. Modell.* **2014**, *283*, 1–7. [CrossRef]
5. Su, S.; Ma, X.; Xiao, R. Agricultural landscape pattern changes in response to urbanization at ecoregional scale. *Ecol. Indic.* **2014**, *40*, 10–18. [CrossRef]
6. Zhao, Z.; Sharifi, A.; Dong, X.; Shen, L.; He, B.-J. Spatial variability and temporal heterogeneity of surface urban heat island patterns and the suitability of local climate zones for land surface temperature characterization. *Remote Sens.* **2021**, *13*, 4338. [CrossRef]
7. Li, H.; Peng, J.; Yanxu, L.; Yi'na, H. Urbanization impact on landscape patterns in Beijing City, China: A spatial heterogeneity perspective. *Ecol. Indic.* **2017**, *82*, 50–60. [CrossRef]
8. He, B.-J.; Zhao, Z.-Q.; Shen, L.-D.; Wang, H.-B.; Li, L.-G. An approach to examining performances of cool/hot sources in mitigating/enhancing land surface temperature under different temperature backgrounds based on landsat 8 image. *Sustain. Cities Soc.* **2019**, *44*, 416–427. [CrossRef]
9. Zhang, H.; Qi, Z.-F.; Ye, X.-Y.; Cai, Y.-B.; Ma, W.-C.; Chen, M.-N. Analysis of land use/land cover change, population shift, and their effects on spatiotemporal patterns of urban heat islands in metropolitan Shanghai, China. *Appl. Geogr.* **2013**, *44*, 121–133. [CrossRef]
10. Zhao, Z.-Q.; He, B.-J.; Li, L.-G.; Wang, H.-B.; Darko, A. Profile and concentric zonal analysis of relationships between land use/land cover and land surface temperature: Case study of Shenyang, China. *Energy Build.* **2017**, *155*, 282–295. [CrossRef]
11. Hassan, T.; Zhang, J.; Prodhon, F.A.; Pangali Sharma, T.P.; Bashir, B. Surface urban heat islands dynamics in response to LULC and vegetation across South Asia (2000–2019). *Remote Sens.* **2021**, *13*, 3177. [CrossRef]
12. Kandel, H.; Melesse, A.; Whitman, D. An analysis on the urban heat island effect using radiosonde profiles and Landsat imagery with ground meteorological data in South Florida. *Int. J. Remote Sens.* **2016**, *37*, 2313–2337. [CrossRef]
13. Dadashpoor, H.; Azizi, P.; Moghadasi, M. Land use change, urbanization, and change in landscape pattern in a metropolitan area. *Sci. Total Environ.* **2019**, *655*, 707–719. [CrossRef]
14. Deng, J.S.; Wang, K.; Hong, Y.; Qi, J.G. Spatio-temporal dynamics and evolution of land use change and landscape pattern in response to rapid urbanization. *Landsc. Urban Plan.* **2009**, *92*, 187–198. [CrossRef]
15. Weng, Y.-C. Spatiotemporal changes of landscape pattern in response to urbanization. *Landsc. Urban Plan.* **2007**, *81*, 341–353. [CrossRef]
16. Kamusoko, C.; Aniya, M. Land use/cover change and landscape fragmentation analysis in the Bindura District, Zimbabwe. *Land Degrad. Dev.* **2007**, *18*, 221–233. [CrossRef]
17. Fan, Q.; Ding, S. Landscape pattern changes at a county scale: A case study in Fengqiu, Henan Province, China from 1990 to 2013. *CATENA* **2016**, *137*, 152–160. [CrossRef]
18. Gorelick, N.; Hancher, M.; Dixon, M.; Ilyushchenko, S.; Thau, D.; Moore, R. Google Earth Engine: Planetary-scale geospatial analysis for everyone. *Remote Sens. Environ.* **2017**, *202*, 18–27. [CrossRef]
19. Hu, Y.; Hu, Y. Land cover changes and their driving mechanisms in Central Asia from 2001 to 2017 supported by Google earth engine. *Remote Sens.* **2019**, *11*, 554. [CrossRef]
20. Hu, Y.; Hu, Y. Detecting forest disturbance and recovery in Primorsky Krai, Russia, using annual Landsat time series and multi-source land cover products. *Remote Sens.* **2020**, *12*, 129. [CrossRef]
21. Qu, L.a.; Chen, Z.; Li, M.; Zhi, J.; Wang, H. Accuracy improvements to pixel-based and object-based lulc classification with auxiliary datasets from Google Earth engine. *Remote Sens.* **2021**, *13*, 453. [CrossRef]
22. McGarigal, K.; Cushman, S.A.; Neel, M.C.; Ene, E. FRAGSTATS: Spatial Pattern Analysis Program for Categorical Maps. Computer Software Program Produced by the Authors at the University of Massachusetts—Amherst. 2002, 6. Available online: www.umass.edu/landeco/research/fragstats/fragstats.html (accessed on 17 September 2022).
23. Piao, Y.; Jeong, S.; Park, S.; Lee, D. Analysis of land use and land cover change using time-series data and random forest in North Korea. *Remote Sens.* **2021**, *13*, 3501. [CrossRef]
24. Herold, M.; Couclelis, H.; Clarke, K.C. The role of spatial metrics in the analysis and modeling of urban land use change. *Comput. Environ. Urban Syst.* **2005**, *29*, 369–399. [CrossRef]
25. Engler, R.; Teplyakov, V.; Adams, J.M. An assessment of forest cover trends in South and North Korea, from 1980 to 2010. *Environ. Manag.* **2014**, *53*, 194–201. [CrossRef]
26. Choi, W.; Kang, S.; Choi, J.; Larsen, J.J.; Oh, C.; Na, Y.-G. Characteristics of deforestation in the Democratic People's Republic of Korea (North Korea) between the 1980s and 2000s. *Reg. Environ. Change* **2017**, *17*, 379–388. [CrossRef]

27. Yu, J.; Park, H.; Lee, S.-H.; Kim, K. Review of slope criteria and forestland restoration plan in North Korea. *J. Korea Soc. Environ. Restor. Technol.* **2016**, *19*, 19–28. [[CrossRef](#)]
28. Park, K.; Lee, S.; Park, S. A study on the North Korea's change of forest policy since the economic crisis in 1990s. *Korean J. Unification Aff.* **2009**, *21*, 459–492.
29. Lim, C.-H.; Choi, Y.; Kim, M.; Jeon, S.W.; Lee, W.-K. Impact of deforestation on agro-environmental variables in cropland, North Korea. *Sustainability* **2017**, *9*, 1354. [[CrossRef](#)]
30. Farr, T.G.; Rosen, P.A.; Caro, E.; Crippen, R.; Duren, R.; Hensley, S.; Kobrick, M.; Paller, M.; Rodriguez, E.; Roth, L.; et al. The shuttle radar topography mission. *Rev. Geophys.* **2007**, *45*. [[CrossRef](#)]
31. DeFries, R.S.; Townshend, J.R.G. NDVI-derived land cover classifications at a global scale. *Int. J. Remote Sens.* **1994**, *15*, 3567–3586. [[CrossRef](#)]
32. McFeeters, S.K. The use of the Normalized Difference Water Index (NDWI) in the delineation of open water features. *Int. J. Remote Sens.* **1996**, *17*, 1425–1432. [[CrossRef](#)]
33. Sulla-Menashe, D.; Friedl, M.A. *User Guide to Collection 6 MODIS Land Cover (MCD12Q1 and MCD12C1) Product*; United States Geological Survey: Reston, VA, USA, 2018; Volume 1, p. 18.
34. Masiliūnas, D.; Tsendbazar, N.-E.; Herold, M.; Lesiv, M.; Buchhorn, M.; Verbesselt, J. Global land characterisation using land cover fractions at 100 m resolution. *Remote Sens. Environ.* **2021**, *259*, 112409. [[CrossRef](#)]
35. Li, C.; Gong, P.; Wang, J.; Zhu, Z.; Biging, G.S.; Yuan, C.; Hu, T.; Zhang, H.; Wang, Q.; Li, X.; et al. The first all-season sample set for mapping global land cover with Landsat-8 data. *Sci. Bull.* **2017**, *62*, 508–515. [[CrossRef](#)]
36. Gong, P.; Wang, J.; Yu, L.; Zhao, Y.; Zhao, Y.; Liang, L.; Niu, Z.; Huang, X.; Fu, H.; Liu, S.; et al. Finer resolution observation and monitoring of global land cover: First mapping results with Landsat TM and ETM+ data. *Int. J. Remote Sens.* **2013**, *34*, 2607–2654. [[CrossRef](#)]
37. Chen, J.; Chen, J.; Liao, A.; Cao, X.; Chen, L.; Chen, X.; He, C.; Han, G.; Peng, S.; Lu, M.; et al. Global land cover mapping at 30m resolution: A POK-based operational approach. *ISPRS J. Photogramm.* **2015**, *103*, 7–27. [[CrossRef](#)]
38. Hansen, M.C.; Potapov, P.V.; Moore, R.; Hancher, M.; Turubanova, S.A.; Tyukavina, A.; Thau, D.; Stehman, S.V.; Goetz, S.J.; Loveland, T.R.; et al. High-resolution global maps of 21st-century forest cover change. *Science* **2013**, *342*, 850–853. [[CrossRef](#)]
39. Oliphant, A.J.; Thenkabail, P.S.; Teluguntla, P.; Xiong, J.; Gumma, M.K.; Congalton, R.G.; Yadav, K. Mapping cropland extent of Southeast and NorthEast Asia using multi-year time-series Landsat 30-m data using a random forest classifier on the Google Earth Engine Cloud. *Int. J. Appl. Earth Obs. Geoinf.* **2019**, *81*, 110–124. [[CrossRef](#)]
40. Jin, Y.; Sung, S.; Lee, D.K.; Biging, G.S.; Jeong, S. Mapping deforestation in North Korea using phenology-based multi-index and random forest. *Remote Sens.* **2016**, *8*, 997. [[CrossRef](#)]
41. Chander, G.; Markham, B.L.; Helder, D.L. Summary of current radiometric calibration coefficients for Landsat MSS, TM, ETM+, and EO-1 ALI sensors. *Remote Sens. Environ.* **2009**, *113*, 893–903. [[CrossRef](#)]
42. Yin, G.; Mariethoz, G.; Sun, Y.; McCabe, M.F. A comparison of gap-filling approaches for Landsat-7 satellite data. *Int. J. Remote Sens.* **2017**, *38*, 6653–6679. [[CrossRef](#)]
43. Inglada, J.; Vincent, A.; Arias, M.; Tardy, B.; Morin, D.; Rodes, I. Operational high resolution land cover map production at the country scale using satellite image time series. *Remote Sens.* **2017**, *9*, 95. [[CrossRef](#)]
44. Foody, G.M.; Mathur, A. Toward intelligent training of supervised image classifications: Directing training data acquisition for SVM classification. *Remote Sens. Environ.* **2004**, *93*, 107–117. [[CrossRef](#)]
45. Talukdar, S.; Singha, P.; Mahato, S.; Shahfahad, Pal, S.; Liou, Y.; Rahman, A. Land-use land-cover classification by machine learning classifiers for satellite observations—A review. *Remote Sens.* **2020**, *12*, 1135. [[CrossRef](#)]
46. Breiman, L. Random forests. *Mach. Learn.* **2001**, *45*, 5–32. [[CrossRef](#)]
47. Naghibi, S.A.; Pourghasemi, H.R.; Dixon, B. GIS-based groundwater potential mapping using boosted regression tree, classification and regression tree, and random forest machine learning models in Iran. *Environ. Monit. Assess.* **2016**, *188*, 44. [[CrossRef](#)]
48. Tamiminia, H.; Salehi, B.; Mahdianpari, M.; Quackenbush, L.; Adeli, S.; Brisco, B. Google Earth Engine for geo-big data applications: A meta-analysis and systematic review. *ISPRS J. Photogramm.* **2020**, *164*, 152–170. [[CrossRef](#)]
49. Rodriguez-Galiano, V.F.; Ghimire, B.; Rogan, J.; Chica-Olmo, M.; Rigol-Sanchez, J.P. An assessment of the effectiveness of a random forest classifier for land-cover classification. *ISPRS J. Photogramm.* **2012**, *67*, 93–104. [[CrossRef](#)]
50. Abdullah, A.Y.M.; Masrur, A.; Adnan, M.S.G.; Baky, M.A.A.; Hassan, Q.K.; Dewan, A. Spatio-temporal patterns of land use/land cover change in the heterogeneous coastal region of Bangladesh between 1990 and 2017. *Remote Sens.* **2019**, *11*, 790. [[CrossRef](#)]
51. Křováková, K.; Semerádová, S.; Mudrochová, M.; Skaloš, J. Landscape functions and their change—A review on methodological approaches. *Ecol. Eng.* **2015**, *75*, 378–383. [[CrossRef](#)]
52. Anderson, J.R. *A Land Use and Land Cover Classification System for Use with Remote Sensor Data*; Government Printing Office: Washington, DC, USA, 1976; Volume 964.
53. Statistics Korea. *Major Statistical Indicators of North Korea*; Major Statistical Indicators of North Korea: Seoul, Republic of Korea, 2020. (In Korean)
54. Lee, S. *North Korean Industrial Statistics*; KIET: Sejong, Republic of Korea, 2015.

55. Oh, S.; Kim, E.; Kim, K. Characteristics of forest policy in the Kim Jong-Un era. *North Korean Stud.* **2018**, *14*, 101–133.
56. National Institute of Forest Science. *Development of a Method of Constructing North Korean Forest Information Using Satellite Imagery and AI*; National Institute of Forest Science: Seoul, Republic of Korea, 2020. (In Korean)

Disclaimer/Publisher's Note: The statements, opinions and data contained in all publications are solely those of the individual author(s) and contributor(s) and not of MDPI and/or the editor(s). MDPI and/or the editor(s) disclaim responsibility for any injury to people or property resulting from any ideas, methods, instructions or products referred to in the content.